

Predictors of Fixation Probability on Complete Networks Involving Multiplayer Interactions Under Coordinated Movement Systems

Hasan Haq1 · Pedro H. T. Schimit2 · Mark Broom1

Accepted: 27 February 2025 © The Author(s) 2025

Abstract

In recent years, classical evolutionary models have been extended to incorporate realistic multiplayer interactions rather than the traditional pairwise modelling approach. Several papers have introduced a new evolutionary framework involving population structure, evolutionary dynamics, multiplayer games and movement processes. The theory underlying the framework has been explored in several directions, identifying strong predictors of fixation probability, such as mean group size and temperature. A recent study developed an evolutionary model where individuals move in a coordinated manner via newly developed movement mechanisms, resulting in herding or separation within the population. This analysis demonstrated that these movement mechanisms impact the fixation probability of cooperation. This paper extends this analysis by investigating whether the previously identified predictors of fixation probability retain their strong influences under different games on complete graphs and by considering a different social dilemma in the form of the Stag-Hunt game. We show that previously defined measures of aggregation are directly related to mean group size and that these fundamental measures can be analytically calculated. In the Stag-Hunt game, we demonstrate that herding opposes the evolution of cooperation. In the Public Goods game, we demonstrate that temperature and fixation share a linear relationship regardless of the movement mechanism considered. In the Hawk-Dove game, temperature is a stronger predictor of fixation but the linear relationship breaks down for higher temperatures and a similar relationship holds as for the Stag-Hunt game.

Keywords Evolutionary game theory \cdot Evolutionary graph theory \cdot Structured populations \cdot Multiplayer games \cdot Predictors \cdot Coordinated movement

Published online: 27 March 2025

Pedro H. T. Schimit schimit@alumni.usp.br

Mark Broom

Mark.Broom.1@citystgeorges.ac.uk

- Department of Mathematics, City St George's, University of London, 10 Northampton Square, ECIV 0HB London, UK
- Informatics and Knowledge Management Graduate Program, Universidade Nove de Julho, Rua Vergueiro, 235/249, 01504-000 São Paulo, SP, Brazil



1 Introduction

Evolutionary graph theory, developed by Lieberman et al. [1], has significantly advanced the modelling of structured populations. Unlike traditional evolutionary game theory models, which assume infinite, homogeneous populations (Maynard Smith [2]), evolutionary graph theory focuses on finite, inhomogeneous populations. This approach allows for more realistic features, such as geographical structure, where individuals are more likely to interact with others in close proximity. In evolutionary graph theory, the population is represented by a graph. Individuals are represented by the vertices of the graph and interact with neighbouring individuals via the edges. These interactions determine the fitness of each member of the population, which plays a central role in the evolutionary dynamics governing the evolution of the population. One of the key advantages of evolutionary graph theory is its ability to incorporate various population structures (Antal and Scheuring [3]; Broom and Rychtar [4]; Maciejewski [5]; Hindersin and Traulsen [6]; Cuesta et al. [7]), and research has shown that graphical topology significantly influences population evolution (Santos and Pacheco [8]; Broom and Rychtar [4]; Broom et al. [9]; Li et al. [10]; Voorhees [11]; Tkadlec et al. [12]; Fic and Gokhale [13]).

However, evolutionary graph theory typically models interactions between individuals as pairwise contests, rather than a more realistic multiplayer approach. A recent series of research papers has addressed this limitation via the development of an extensive modelling framework that examines the evolution of structured populations where individuals engage in multiplayer contests, which we refer to as the Broom-Rychtár framework (Broom and Rychtar [14], Broom et al. [15]; Broom et al. [16]). Evolutionary multiplayer games were introduced by Palm [17], and the theory was developed by Broom et al. [18], see also Bukowski and Miekisz [19]. These interactions often use standard games such as Public Goods, Hawk-Dove and the Stag-Hunt (Ohtsuki et al. [20]; Santos et al. [21]; van Veelen and Nowak [22]; Hadjichrysanthou et al. [23], Broom and Rychtar [24]). The framework has been explored in various directions (Broom et al. [15]; Pattni et al. [25]; Schimit et al. [26]; Schimit et al. [27]), but a significant class of models was considered in Broom et al. [15] where the population was represented by a territorial raider model (a special case of the Broom-Rychtár framework).

In Broom et al. [15], individuals can move and interact in arbitrary group sizes under the BDB dynamics (invasion process), where an individual is first selected to reproduce with probability proportional to the fitness they accrue from their interactions, relative to the total of the fitnesses within the population. Following this, a replacement event occurs, in which the offspring randomly replaces another member of the parent's group as explained in section 3.2. In this and several other models, individuals move independently i.e. without influence from past movements (history-independent) nor from the movement of other individuals (row-independent), see Broom et al. [15]; Schimit et al. [26]; Schimit et al. [27]. Other types of movement, such as history-dependent movement, where present movement decisions are affected by past movements have also been considered (Pattni et al. [28]; Erovenko et al. [29]). What was missing from the existing literature, however, was the consideration of row-dependent movement in the evolution of cooperative behaviour, where the movements of individuals are influenced by the movement of others.

In Broom et al. [30], various row-dependent movement models were developed to characterise realistic movement behaviours, such as migration, herding, and dispersal. In Haq et al. [31], these movement procedures were incorporated in the evolutionary setting of the territorial raider model through the development of a generalised movement modelling approach, demonstrating how individuals could achieve an apriori target distribution. The



effects of the movement mechanisms on the evolution of cooperation in the Public Goods and Hawk-Dove games on complete networks were extensively explored. However, it has been previously shown that measures such as mean group size and temperature are strong predictors of fixation probability, with temperature often being the stronger predictor (Broom et al. [15]; Schimit et al. [26]; Schimit et al. [26]). The purpose of this paper is to extend the previous analysis by using the evolutionary model developed in Haq et al. [31] to investigate how the row-dependent movement mechanisms affect the predictors of fixation probability, and whether the measures retain their significance as strong predictors of fixation. We also consider the Stag-Hunt game as this has not been previously considered, to investigate the effects of row-dependent movement in a social dilemma game where selection can potentially favour cooperation.

2 The Broom-Rychtár Framework

The modelling framework developed by Broom and Rychtar [14] acts as the theoretical foundation for work that has been extensively explored (Broom et al. [32]; Erovenko et al. [29]; Erovenko and Broom. [33]) and the work done in this paper. The key components of the framework are: the population structure, the evolutionary dynamics and the multiplayer games. The fully independent model was developed from this framework, and was extended to the territorial raider model which we use within this paper.

3 The Model

In Haq et al. [31], a model was developed that combined the evolutionary setting of the territorial raider model from Broom et al. [15] with the movement mechanisms from Broom et al. [30]. This model is the basis for the work done in this paper and we first explain its four key components: population structure, evolutionary dynamics, multiplayer games and movement procedures.

3.1 Population Structure: Territorial Raider Model

The most significant example of the Broom-Rychtar framework is the territorial raider model (illustrated in Fig.1), which has been extensively explored (Broom et al. [15]; Pattni et al. [25]; Schimit et al. [26]). In the territorial raider model, there are N individuals who move and interact with other individuals at M places. Individual I_i lives at place P_m throughout the entire evolutionary process. In the original territorial raider model from Broom and Rychtar [14] there was a one-to-one correspondence between individuals and places, although this was generalised in Pattni et al. [25]. The global home fidelity parameter h is a measure of the preference individuals have for staying on their home vertex and is the same for all individuals. The higher h is, the more likely individuals are to stay on their home vertex and, therefore, less likely to move and interact with other individuals. Given an individual I_i with m neighbouring places, the probability of I_i staying home is h/(h+m) and moving is m/(h+m). If h=1, this represents an indifference individuals have between all reachable places and means that they are equally likely to visit any of them and if the base graph is the complete graph, this is a completely mixed population.



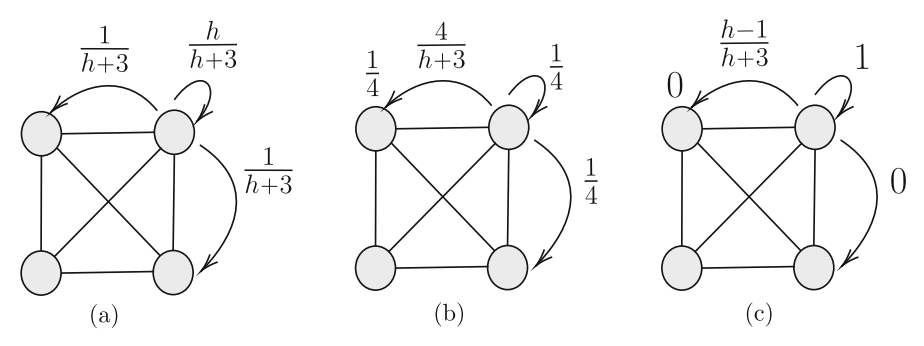


Fig. 1 The territorial raider model of Broom and Rychtar [14]. **a** Population structure is represented using a complete graph with 4 nodes. Individual I_n lives in place P_m and can visit any neighbouring place. The apriori distribution for any individual is $P(I_n)$ is on their home vetex $P_m = \frac{h}{h+3}$ and $P(I_n)$ is elsewhere $P_m = \frac{3}{h+3}$. **b** $P_m = \frac{3}{h+3}$. **b** $P_m = \frac{3}{h+3}$ is movement distribution is represented using the movement methodology explained in section 3.5 where the $P_m = \frac{3}{h+3}$ in the movement process. **c** using the methodology in section 3.5, $P_m = \frac{3}{h+3}$ in the movement process and, therefore, stays on their home vertex. Thus the process in (a) is represented by an individual following (b) with probability $P_m = \frac{h}{h+3}$ and (c) with probability $P_m = \frac{h}{h+3}$

Individuals move along the graph according to their own movement distributions and form groups on the vertices of the graph. Let G denote a group of individuals; then $\chi(m, G)$ represents the probability of group G forming at place P_m . When groups of individuals are formed, multiplayer contests are played. Individual I_n receives a payoff that depends upon the composition of the group G itself and the place P_m the group is located in, denoted by $R_{n,m,G}$. Individual I_n 's average fitness is calculated by considering all payoffs they can receive averaged over all possible groups and places,

$$F_n = \sum_{m} \sum_{\substack{G \\ n \in G}} \chi(m, G) R_{n,m,G}. \tag{1}$$

3.2 Evolutionary Dynamics

In this paper, the evolutionary process is governed by an invasion process (Lieberman et al. [1], Nowak [34]), a birth death process in which selection acts on the first event (written BDB or Bd), which has been commonly used in evolutionary graph theory, and adapted to the Broom-Rychtá \hat{r} framework in Broom et al. [15].

An individual I_i is first selected to reproduce with probability proportional to their fitness i.e.

$$b_i = \frac{F_i}{\sum_k F_k}. (2)$$

Then the offspring replaces another individual I_i with probability

$$d_{ij} = \begin{cases} \sum_{m} \sum_{G} \frac{\chi(m,G)}{|G|-1}, & i \neq j, \\ \sum_{i,j \in G} \sum_{m} \chi(m,\{i\}), & i = j \end{cases}$$
 (3)

The replacement probability assumes that an offspring of individual I_i will replace individual I_i with probability proportional to the time I_i and I_i spend with each other. The offspring of I_i can also replace its parent I_i , and it does so with probability proportional to the time I_i spends alone. This is because if an isolated individual is selected to reproduce, its offspring is guaranteed to replace the parent, as there are no other individuals available for replacement. An alternative explanation is that as there are no individuals for the offspring to replace, it does not survive and the parent is not replaced. In either case the population is effectively unchanged. When $i \neq j$, the probability of individuals I_i and I_j meeting is given by summing all $\chi(m,\mathcal{G})$ over all m such that $I_i, I_i \in G$. We assume that I_i spends an equal amount of time with all other members of group \mathcal{G} , therefore we weight by $1/(|\mathcal{G}|-1)$ as there are $|\mathcal{G}|-1$ other members of the group. However, when i=j, we sum $\chi(m,\mathcal{G})$ over all m such that $\mathcal{G} = \{i\}$. There is no need to weight $\chi(m, \mathcal{G})$ because I_i is alone.

The temperature of an individual was derived in Lieberman et al. [1]; it is proportional to the likelihood of an individual being replaced within a neutral population where all members have constant fitness. The temperature is given by

$$\tau_j = \sum_{i \neq j} d_{ij}. \tag{4}$$

The higher the temperature of an individual, the more likely they are to be replaced. Note that, as in Haq et al. [31], we only consider complete networks, and so can write d_{ij} as d_N (since d depends upon N). All individuals then have the same temperature and this can be expressed as

$$\tau_N = (N-1)d_N. \tag{5}$$

3.3 The Fixation Probability

The fixation probability is regarded as the most significant measure within a finite evolutionary system as it measures the likelihood of the evolutionary success of a particular strategy. The fixation probability $\rho^{\mathcal{C}}(\rho^{\mathcal{D}})$ is the probability that the offspring of a randomly placed mutant cooperator (defector) eventually replaces the entire population. In the Stag-hunt game, we use $\frac{1}{N}$ as a benchmark when comparing fixation probabilities. As explained in Taylor et al. [35], we say that selection favours cooperators replacing defectors when $\rho^{\mathcal{C}} > \frac{1}{N}$, and cooperation evolves if $\rho^{\mathcal{C}} > \frac{1}{N} > \rho^{\mathcal{D}}$.

In Haq et al. [31], it was shown that by using standard results from Karlin and Taylor [36], the fixation probability of a mutant cooperator (in the Public Goods game) and dove (in the Hawk-Dove game) under BDB dynamics on a complete N-sized network are respectively given by

$$\rho^{\mathcal{C}} = \frac{1}{1 + \sum_{i=1}^{N-1} \prod_{k=1}^{j} \frac{R + kV d_{N}}{R - C + (k-1)V d_{N}}},\tag{6}$$

$$\rho^{\mathcal{C}} = \frac{1}{1 + \sum_{j=1}^{N-1} \prod_{k=1}^{j} \frac{R + kV d_N}{R - C + (k - 1)V d_N}},$$

$$\rho^{\mathcal{D}} = \frac{1}{1 + \sum_{j=1}^{N-1} \prod_{k=1}^{j} \frac{R + \omega V - \nu C}{R + \tau V}}.$$
(6)

Here, R corresponds to the background payoff individuals receive from activities unrelated to the games, V represents the reward individuals gain from the multiplayer contests and C is the cost individuals endure from the contests. These variables are described in more detail in Section (3.4). We used these formulae (6) and (7) in our analysis to demonstrate the underlying relationship between temperature and fixation probability.



3.4 Multiplayer Games in Structured Populations

We considered three different multiplayer games to describe the interactions between individuals. The Public Goods, Hawk-Dove and Stag-Hunt games. Each of the games describes a contest between two different types of individuals, A and B. Using these games, we describe an evolutionary process of a single mutant cooperator within a population of resident defectors. In the payoffs described for each of the games, R is the background payoff individuals receive from activities unrelated to the games, C represents the cost and V is the reward gained.

3.4.1 The Multiplayer Public Goods Game

In this game individuals can either cooperate (A) or defect (B). The cooperator pays a cost which is shared among the rest of the group as a reward but not shared by the individual who made the sacrifice. Defectors pay no cost. After a game is played between a group of x cooperators and y defectors, the payoffs are respectively

$$R_{x,y}^{\mathcal{A}} = \begin{cases} R - C, & x = 1\\ R - C + \left(\frac{x - 1}{x + y - 1}\right)V, & x > 1 \end{cases}$$
 (8)

$$R_{x,y}^{\mathcal{B}} = \begin{cases} R, & x = 0\\ R + \left(\frac{x}{x+y-1}\right)V, & x > 0 \end{cases}$$

$$\tag{9}$$

3.4.2 The Multiplayer Hawk-Dove Game

In the Hawk-Dove game, individuals compete for resources located on the vertices. Doves (\mathcal{B}) will always share the reward amongst all other individuals unless there are hawks (\mathcal{A}) present within the group. In this case, doves will concede and hawks will compete amongst themselves for the reward. A single hawk wins the reward, while all other hawks endure a cost from the violent contest. In a group of x hawks and y doves, the average payoffs are given by

$$R_{x,y}^{\mathcal{A}} = R + \frac{V - (x-1)C}{x}$$
 (10)

$$R_{x,y}^{\mathcal{B}} = \begin{cases} R, & \text{if } x > 0\\ R + \frac{V}{y} & \text{if } x = 0 \end{cases}$$
 (11)

3.4.3 The Multiplayer Stag-Hunt Game

The multiplayer Stag-Hunt game consists of two types of individuals, cooperators (A) and defectors (B). The payoff functions are step functions where L>1 cooperators are required to group together for the public good to be produced. The cooperators always pay a cost C regardless of whether the threshold is met or not. In a group of x cooperators and y defectors, the payoffs are given by

$$R_{x,y}^{\mathcal{A}} = \begin{cases} R - C, & x < L \\ R - C + \left(\frac{x}{x+y}\right)V, & x \ge L \end{cases}$$
 (12)

$$R_{x,y}^{\mathcal{B}} = \begin{cases} R, & x < L \\ R + \left(\frac{x}{x+y}\right)V, & x \ge L \end{cases}$$
 (13)

3.5 The Movement Process

In Haq et al. [31] a general movement methodology was developed that embeds the row-dependent movement models from Broom et al. [30] into the evolutionary setting of the territorial raider model which we use within this paper. The methodology consists of a probability distribution that describes the various movement decisions available to individuals within the population. This includes both those who partake in the movement process (governed by the chosen row-dependent movement mechanism) and those who do not, with the actions available for the latter group varying according to the value of h. Consider a complete graph where there are M places.

- If h > 1, then an individual can either partake in the process and move via the movement mechanism with probability $\frac{M}{h+M-1}$ or they do not move and stay at their home vertex with probability $\frac{h-1}{h+M-1}$.
- If h = 1, then every member of the population plays the process.
- If h < 1, then an individual can either move via the process with probability $\frac{Mh}{h+M-1}$ or they move to a random non-home place with probability $\frac{(M-1)(1-h)}{h+M-1}$.

The main purpose of this approach was to achieve a target distribution given by an apriori distribution, denoted by a_m , which represents the probability of a randomly selected individual going to a particular place. However, we omit the details which can be found in Haq et al. [31]. When individuals partake in the movement process, they will move via one of the three mechanisms: *follow the majority, Polya-urn*, or *the wheel*. Note that the first step of the sequential movement processes (follow the majority and Polya-urn) is to assign the ordering uniformly at random over all possible orderings (or if simulating a large population, make selection among the remaining individuals at each step of the sequence with uniform probability). Using this methodology, important metrics such as the mean group size and temperature can be calculated which we show in Sect. 4.1.

In Broom and Rychtar [14], the mean group size from the individual's perspective was found to be

$$\bar{G} = \sum_{m} \sum_{G} \frac{\chi(m, G)|G|^2}{\sum_{m} \sum_{G} \chi(m, G)|G|}.$$
 (14)

Broom et al. [30] derived novel measures of aggregation which we can also calculate using the methodology described above. The most significant of these measures was denoted as T which is the probability of two individuals being together which is one of the most fundamental properties of any movement process which is given by

$$T = \frac{1}{N(N-1)} \sum_{m=1}^{M} E[X_m(X_m - 1)], \tag{15}$$

where X_m denotes the number of individuals on place P_m .



3.6 Follow the Majority

The type of coordinated movement we first consider is the *follow the majority* process where individuals simply move to the place that provides them with the most utility. The first individual moves to a place according to its apriori distribution and subsequent individuals simply move to the place where the largest number of individuals reside. The utility an individual receives from place P_m is given by

$$U_m = Y_m + 1, (16)$$

where Y_m is the current number of occupants on place P_m . For a well-mixed population on a complete graph with h = 1, this results in all individuals being in a single group on the same vertex, the location of which follows the apriori distribution.

3.7 The Polya-urn

The Polya-urn model represents a probabilistic movement process, where individuals move to a place with probability relative to their utility function i.e. an individual moves to place P_m with probability $U_m / \sum_k U_k$. This probabilistic model is represented by an urn model (Johnson and Kotz [37]), where balls are numbered 1, 2, ..., M and placed into an urn and then sequentially drawn out at random. The n^{th} ball with number m being drawn out corresponds to the n^{th} individual moving to place P_m . Utility positively correlates with place occupancy therefore, an extra ball with the same number is placed back into the urn. This translates to the following utility function

$$U_m = Ba_m + Y_m \tag{17}$$

where $B \in (0, \infty)$ corresponds to the initial number of balls in the urn, and a_m is the individual's apriori distribution. Note that as we are selecting the place following a probability distribution rather than picking out balls, B does not need to be integer-valued.

3.8 The Wheel and Base Model

The wheel and base model simultaneously allocates all individuals partaking in the movement process. Assume a base disc of perimeter 1 is divided into M place $P_1, ..., P_M$ in the shape of wedges where P_m has perimeter length a_m see Fig. 2a such that $\sum_m a_m = 1$. On top of the base disc, is an upper disc, the wheel, representing the N individuals in the form of N spikes; see Fig. 2b. The angle between individuals I_i and I_j is given by $2\pi \theta_{ij}$, where $\theta_{ij} \in [-1/2, 1/2]$ can possibly be determined via a probability distribution. Note that $\theta_{ij} = -\theta_{ji}$. When the angles between the spikes have been set, the wheel is spun and rotates by an angle of θ selected uniformly at random. Then, individual I_i moves to place P_m if and only if the corresponding spike lands above the corresponding segment; see Fig. 2c.

The wheel was designed as a simple, idealised model of simultaneous allocation, enabling the construction of distributions with specific properties. For instance, when h=1 and $\theta=2\pi/N$, all individuals in the population are alone, representing a movement process where all individuals simultaneously move and eventually become separated. One could imagine a population of animals moving dispersing from a central location with particular requirements for levels of separation from others. This movement mechanism offers the greatest flexibility and provides a clearer representation of complete aggregation amongst individuals ($\theta=0$).



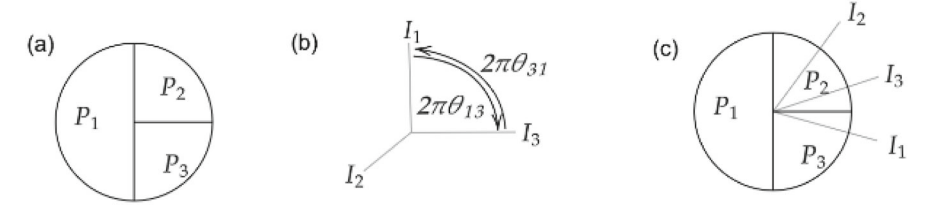


Fig. 2 a M=3 places with $a_1=\frac{1}{2}$, $a_2=\frac{1}{4}$, $a_3=\frac{1}{4}$. **b** represents the N=3 individuals as spikes. The angle between individuals I_i and I_j is given by $2\pi\theta_{ij}$. In this case, $\theta_{13}=\frac{1}{4}=-\theta_{31}$. **c** shows the simultaneous placement of all individuals after the upper disc is spun on top of the base. In this case, individuals I_1 , I_2 , I_3 move to places P_3 , P_2 , P_2 respectively

4 Results

In this section, we first demonstrate how to calculate significant evolutionary predictors of fixation probability. We then present simulation results on fixation probabilities for mutant cooperative strategies from the games defined in Sect. 3.4, under the coordinated movement mechanisms described in section 3.5, and their relationships with mean group size and temperature in a well-mixed population on the complete decagon. This is followed by an analytical explanation for certain trends observed in the simulations.

4.1 Evolutionary Measures Impacting the Fixation Probability

We first considered how T (15) relates to the expected group size. From (14), the expected group size is given by

$$E[|G|] = \frac{E[X_m^2]}{E[X_m]} = E[X_m^2], \tag{18}$$

since as we only considered well-mixed populations on complete graphs where each individual resides within their unique home vertex, the expected number of individuals on a given place is one i.e. $E[X_m] = 1$. By substituting (18) into (15) and simplifying,

$$T = \frac{1}{N-1} (E[|G|] - 1). \tag{19}$$

(19) demonstrates that the aggregation measure T is directly related to the mean group size and if either T or E[|G|] is known, the other can be calculated.

We analytically calculated the evolutionary measures considered in this paper on an N-sized complete network, for h > 1, under the follow the majority, independent and wheel processes. As an example, we show how we calculated the mean group size under follow the majority. Here

$$|G| = \sum_{L=0}^{N} (\lambda)^{L} (1-\lambda)^{N-L} {N \choose L} \left(\frac{N-L}{N} \left(\frac{(L+1)^{2}+N-L-1}{N} \right) + \frac{N}{L} \left(\frac{L^{2}+N-L}{N} \right) \right),$$

$$= \sum_{L=0}^{N} (\lambda)^{L} (1-\lambda)^{N-L} \left({N \choose L} + \frac{1}{N} {N \choose L-1} + \frac{L^{2}(N-2)}{N} {N \choose L} \right),$$

$$= 1 + \lambda \left(1 + (1-\frac{2}{N})((N-1)\lambda + 1) \right)$$
(20)



where $\lambda = \frac{N}{h+N-1}$. By using similar methods, the mean group size under independent movement is given by

$$|G| = 1 + \lambda \left(2 - \frac{1}{N}(2 + \lambda N - \lambda)\right),\tag{21}$$

and the mean group size for the wheel is given by

$$|G| = 1 + \frac{1}{N} \left(\left(\sum_{\lfloor \frac{2\pi}{N\theta} \rfloor}^{N} \left((\lfloor \frac{2\pi}{N\theta} \rfloor)^{2} + \frac{1}{2} ((\lfloor \frac{2\pi}{N\theta} \rfloor)^{2} + \lfloor \frac{2\pi}{N\theta} \rfloor) \left(\frac{N\theta}{2\pi} (1 - \lfloor \frac{2\pi}{N\theta} \rfloor) - 1 \right) + \sum_{L=2}^{\lfloor \frac{2\pi}{N\theta} \rfloor - 1} \left(L^{2} + \frac{L^{2} + L}{2} (\frac{N\theta}{6\pi} (1 - L) - 1) \right) \right) (\lambda)^{L} (1 - \lambda)^{N-L} \binom{N-2}{L-2} + \frac{2(\lambda - \lambda^{2})}{N} \right).$$
(22)

The calculations for (21) and (22) can be found in the appendix leading to the above, labelled (31) and (34).

By using (19), we were able to calculate T for the movement processes by using (20), (21) and (22). For the follow the majority process

$$T = \frac{1}{N-1} \lambda \left(1 + (1 - \frac{2}{N})((N-1)\lambda + 1) \right). \tag{23}$$

Similarly, T under independent movement is given by

$$T = \frac{1}{N-1} \lambda \left(2 - \frac{1}{N} (2 + \lambda N - \lambda) \right), \tag{24}$$

and T for the wheel is

$$T = \frac{1}{N(N-1)} \left(\left(\sum_{\lfloor \frac{2\pi}{N\theta} \rfloor}^{N} \left(\left(\lfloor \frac{2\pi}{N\theta} \rfloor \right)^{2} + \frac{1}{2} \left(\left(\lfloor \frac{2\pi}{N\theta} \rfloor \right)^{2} + \lfloor \frac{2\pi}{N\theta} \rfloor \right) \left(\frac{N\theta}{2\pi} (1 - \lfloor \frac{2\pi}{N\theta} \rfloor) - 1 \right) + \sum_{L=2}^{\lfloor \frac{2\pi}{N\theta} \rfloor - 1} \left(L^{2} + \frac{L^{2} + L}{2} \left(\frac{N\theta}{6\pi} (1 - L) - 1 \right) \right) (\lambda)^{L} (1 - \lambda)^{N-L} \binom{N-2}{L-2} + \frac{2(\lambda - \lambda^{2})}{N} \right).$$

$$(25)$$

To calculate the temperature, we considered an N-sized, well-mixed population and all of the possible ways two individuals I_i and I_j can replace each other within an L-sized group and used the relation $\tau_N = (N-1)d_N$. We show how we calculated this measure under the follow the majority process (the calculations for independent movement and the wheel can be found in the appendix leading to (35), (36) and (37). A group of size L can form in one of three ways:

- I_i and I_j move with L-2 individuals to an empty vertex;
- I_i moves with L-2 individuals to I_j 's home vertex or vice-versa;
- I_i and I_j move with L-3 individuals to a place containing an individual.

We then obtain the following expression where the first summation represents the first two cases and the second summation represents the third case.

$$\tau_N = N - 1 \left(\sum_{L=2}^{N} (\lambda)^{L-2} (1-\lambda)^{N-L} {N-2 \choose L-2} \left(\frac{1}{N} \right) \left(\frac{L}{L-1} (\lambda)^2 + 2\lambda (1-\lambda) \right) \right)$$

$$+\sum_{L=3}^{N} (\lambda)^{L-1} (1-\lambda)^{N-L+1} \binom{N-2}{L-3} \left(\frac{1}{L-1} - \frac{1}{N} \right) ,$$

where $\lambda = \frac{N}{h+N-1}$. By expanding the summations and simplifying, the temperature for follow the majority process on a complete *N*-sized network is given by

$$\tau_N = \lambda + \frac{1 - \lambda}{N} - \frac{(1 - \lambda)^{N - 1}}{N}.$$
 (26)

Using similar methods, the temperature under independent movement is given by equation (27), while the temperature for the wheel is provided in Eqs. (28) and (29).

$$\tau_N = 1 - \frac{(N + N\lambda(\lambda - 1) - \lambda^2)(N - \lambda)^{N-2}}{N^{N-1}}.$$
 (27)

 $0 \le \theta \le \frac{\pi}{N}$:

$$\tau_N = 1 - \left(\frac{1}{N}(N-1)(1-\lambda)(1-(1-\lambda)^{N-1}) + (1-\lambda)^N + \frac{\theta}{\pi}\left(\lambda + \frac{1}{2}((1-\lambda)(1-(1-\lambda)^{N-1}) + (N-1)(\lambda-1)(\lambda))\right)\right).$$
(28)

 $\frac{\pi}{N} \le \theta \le \frac{2\pi}{N}$:

$$\tau_{N} = 1 - \left(\frac{1}{N} \left(-1 + (1 - \lambda)^{N} + \lambda(\lambda + 2) - N(\lambda^{2} + \lambda - 1) \right) - \frac{\theta}{2\pi} \left(-1 + (1 - \lambda)^{N} + \lambda(N + 3\lambda - 3N\lambda) \right) \right).$$
 (29)

The detailed calculations for (27), (28) and (29) can be found in the appendix (35), (36) and (37).

In Broom et al. [15], it was identified that temperature and fixation probability share a linear relationship. This was observed under conditions of high home fidelity and independent movement. However, our analysis in section 4.2 demonstrates that this result generalises across all values of h and for all movement processes. To support this analytically, Haq et al. [31] showed that the fixation probability of a mutant cooperator on a complete N-sized network under BDB dynamics is given by (6). Using the definition of the temperature from (5), we can re-express (6) in terms of the temperature

$$\rho_1^{\mathcal{A}} = \frac{1}{1 + \sum_{j=1}^{N-1} \prod_{k=1}^{j} \frac{R + kV(\frac{T_N}{N-1})}{R - C + (k-1)V(\frac{T_N}{N-1})}}.$$
(30)

(30) shows that by simply knowing the temperature, the cooperator's fixation probability can be calculated, without knowing the governing movement mechanism. Therefore, in the models considered in this paper for the Public Goods game, temperature matters more than the governing movement mechanism and is the most significant measure in the evolutionary process.

Similarly, in Haq et al. [31], it was shown that under independent movement, the fixation probability of a mutant dove on a complete N-sized network is given by (7). It is clear that unlike (6), the fitnesses cannot be expressed in terms of d_N and, therefore, cannot be reexpressed in terms of the temperature. This implies that the governing movement procedure



plays a more significant role in the Hawk-Dove game than in the Public Goods game, hence the presence of the non-linear trends in Fig. 7. A similar analysis holds for the Stag-Hunt game, where the fitnesses will not simply depend on d_N , but other significant factors such as the threshold value.

4.2 Numerical Results

In this section, we conducted similar simulation methods to those used in Haq et al. [31] to investigate evolutionary processes involving the games defined in Sect. 3.4 and whether mean group size (14) and temperature (4) continue to serve as strong predictors of fixation, under models involving row-dependent movement.

One simulation is delineated as follows:

- The decagon complete network is formed using the iGraph library (Csardi and Nepusz [38]).
- The mutant is randomly placed on one of the vertices.
- Every individual moves (or not) from their home vertex according to the model as described in Sect. 3.5. Groups are formed and multiplayer games are played.
- Individuals return to their home places.
- Each individual moves (or not) and groups are formed and the dynamic process occurs.
 No games are played. Instead, one individual is selected to reproduce an offspring that will replace another random member of the group (or its parent if the parent is alone) explained in Sect. 3.2.
- The simulation ends once the mutant fixates in the population or becomes extinct.
- This process is averaged over 1,000,000 cases to minimise statistical variability.

Figure 3 illustrates the fixation probability of a mutant cooperator and defector in the staghunt game under the Polya-urn and wheel processes on the complete decagon. Figure 3a and b show that for the Polya-urn processes where $B \neq 0$, the cooperator's fixation probability reaches its maximum when h = 1, meaning that all members of the population participate in the movement process. This leads to the formation of groups of varying sizes that reach the threshold, enabling members to share the reward among themselves. At this point, the cooperator's fixation probability exceeds 1/N = 0.1, whereas Fig. 3e indicates that the corresponding fixation probability for the defector remains below 1/N. This demonstrates the significant impact of row-dependent movement in the Stag-Hunt game, as it can raise the cooperator's fixation probability not only above neutrality but also above the defector's, thereby facilitating the evolution of cooperation. Corresponding figures are shown in Haq et al. [31] for the Public Goods game. It was shown that under this social dilemma game, cooperation is always below neutrality for all movement processes. However, the results in the Stag-Hunt game demonstrate a stronger influence of the movement mechanisms, as these can raise the cooperator's fixation probability not only above neutrality, but also above the defector's. This is due to the nature of the stag-hunt game, where cooperators can generate rewards when in groups that reach the threshold. However, in the public goods game, defectors always benefit from the presence of cooperators, regardless of whether the threshold is met, thereby undermining the advantages of cooperative behaviour.

We see a similar trend in Fig. 3c and g which show an important example where the wheel process significantly influences the evolution of cooperation. When h = 1 and $\theta = \pi/10$, the cooperator's fixation probability is above 0.15, whereas the defector's corresponding fixation probability is below 0.02. This angle proves very beneficial for cooperators and allows them to meet each other in pairwise groups that meet the threshold to produce the reward. Under



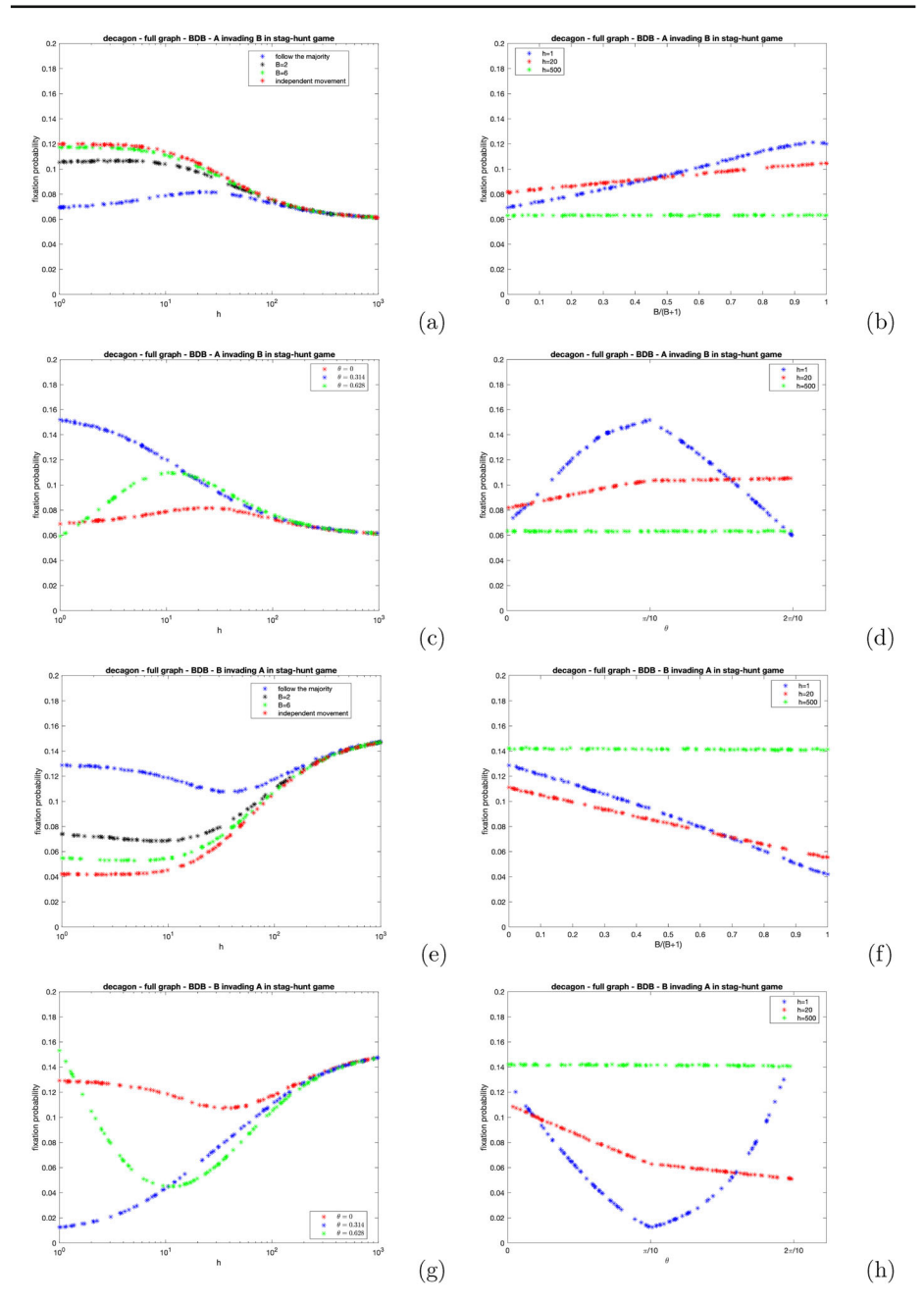


Fig. 3 The fixation probabilities of the cooperator and defector in the stag-hunt game on the complete decagon under the Polya-urn and wheel processes. (the payoffs are set as R=10, C=1, V=12 and L=2). (a), (b), (c) and (d) show the fixation probability of a mutant cooperator in a population of defectors and vice-versa for (e), (f), (g) and (h). Figures (a), (b), (c) and (d) represent the cooperator's fixation probability and figures (e), (f), (g) and (h) represent the defector's. For the Polya-urn, in (a) and (e) we set B=0 (follow the majority), B=2, B=6 and B=10,000 (a sufficiently large value to mirror independent movement). For the wheel, in (c) and (g) we set $\theta=0$ (follow the majority), $\theta=\frac{2\pi}{N}$ (represents a near complete dispersal process), $\theta=\frac{\pi}{N}$. For (b) and (f), we plot the fixation probability against θ (for the Polya-urn) and set $\theta=1$, $\theta=1$ and $\theta=1$ 0. For (d) and (h), we plot the fixation probability against θ (for the wheel) and set $\theta=1$, $\theta=1$ 0 and $\theta=1$ 0. Birkhäuser

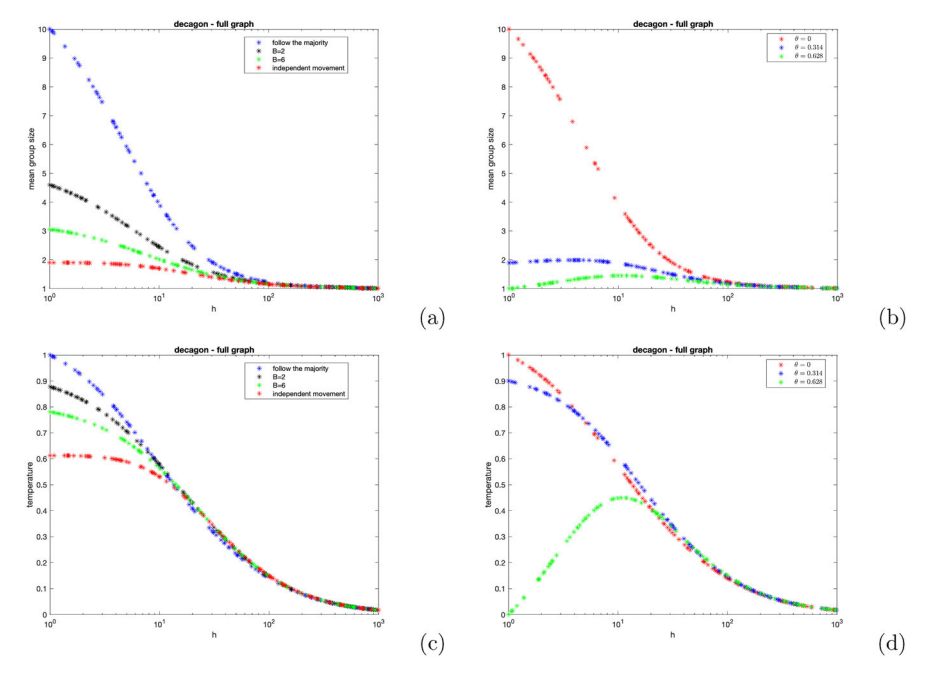


Fig. 4 The mean group size and temperature of individuals within the a well-mixed population on the complete decagon for varying h under distinct Polya-urn processes and wheel processes. (**a**) and (**b**) show the mean group size and (**c**) and (**d**) show the temperature. We set B=0 (follow the majority), B=2, B=6 and B=10,000 (a sufficiently large value of B representing independent movement). We also set $\theta=0$ (follow the majority), $\theta=\frac{2\pi}{N}$ (represents a near complete dispersal process) and $\theta=\frac{\pi}{N}$

these conditions, defectors mostly find themselves in pairwise groups that either contain another defector or a single cooperator, in either case, the reward cannot be produced and the defector's fitness remains relatively low. Therefore, there is a significant disparity between the cooperator's and defector's fixation probabilities.

As *h* increases, the cooperator's fixation probability gradually decreases. This is due to individuals being more likely to remain on their home vertex and, therefore, less likely to move and interact with one another. Therefore, the likelihood of cooperators being in groups where the threshold is reached diminishes, while defectors have a higher relative fitness when all individuals are alone, thereby reducing the cooperator's fixation probability.

For the follow the majority process (B=0), the cooperator's fixation probability is at its lowest compared to the other movement processes. This is due to all members partaking in the movement process aggregating on the same vertex, allowing defectors to exploit cooperators by receiving a share of the produced reward without incurring any cost. Under this movement process, defectors have a greater relative fitness than cooperators, thereby minimising the cooperator's fixation probability. An important result in this context is that herding proves quite detrimental to cooperators, as it reduces their fixation probability below the neutral benchmark of $\frac{1}{N}$ and raises the defector's above this level, thereby favouring the evolution of defection. As h rises, the fixation probability gradually rises, as individuals are more likely to be in smaller groups, until h reaches a level where individuals are most inclined to remain on their home vertex. As h continues to increase, the fixation probability falls as cooperators are



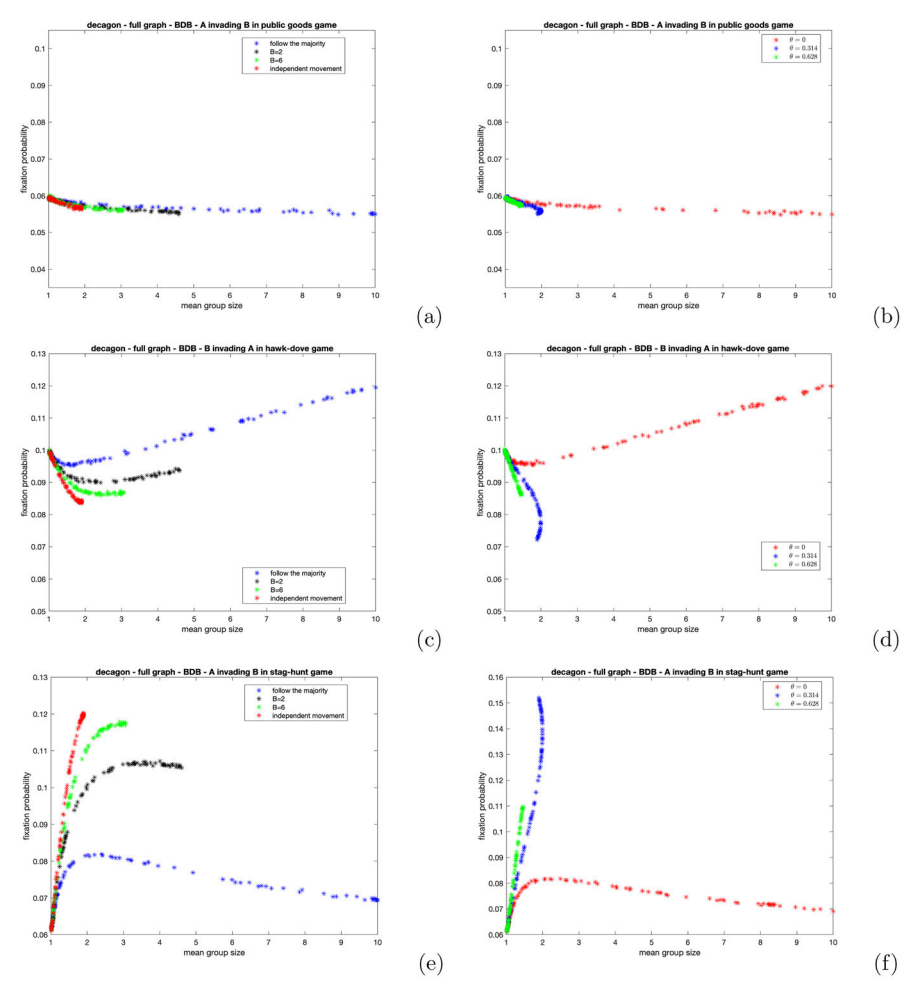


Fig. 5 The fixation probability plotted against the mean group size for a well-mixed population in the Public Goods, Hawk-Dove and Stag-Hunt games on the complete decagon graph. As we vary h, we plot the corresponding fixation probability and mean group size values against each other. Figures (**a**), (**c**) and (**e**) illustrate Polya-urn processes where we set B=0 (follow the majority), B=2, B=6 and B=10,000 (a sufficiently large value of B representing independent movement). (**b**), (**d**) and (**f**) show wheel processes where we set $\theta=0$ (follow the majority), $\theta=\frac{2\pi}{N}$ (represents a near complete dispersal process) and $\theta=\frac{\pi}{N}$

always alone and continue to pay a cost, unlike defectors who do not and, therefore, maintain a higher relative fitness.

Figure 4 illustrates the mean group size and temperature under distinct Polya-urn and wheel processes for varying values of h on the complete decagon graph. In Fig. 4a, the mean group size reaches its maximum when h=1 across all movement processes. This is because all individuals participate in the movement process at this value of h, meaning that under the follow the majority process, the mean group size is equal to the population size. However, as the value of B increases, the value of the mean group size decreases. This is due to the movement process gradually shifting from a deterministic type to a stochastic process, eventually becoming a completely random movement process as the number of balls in the



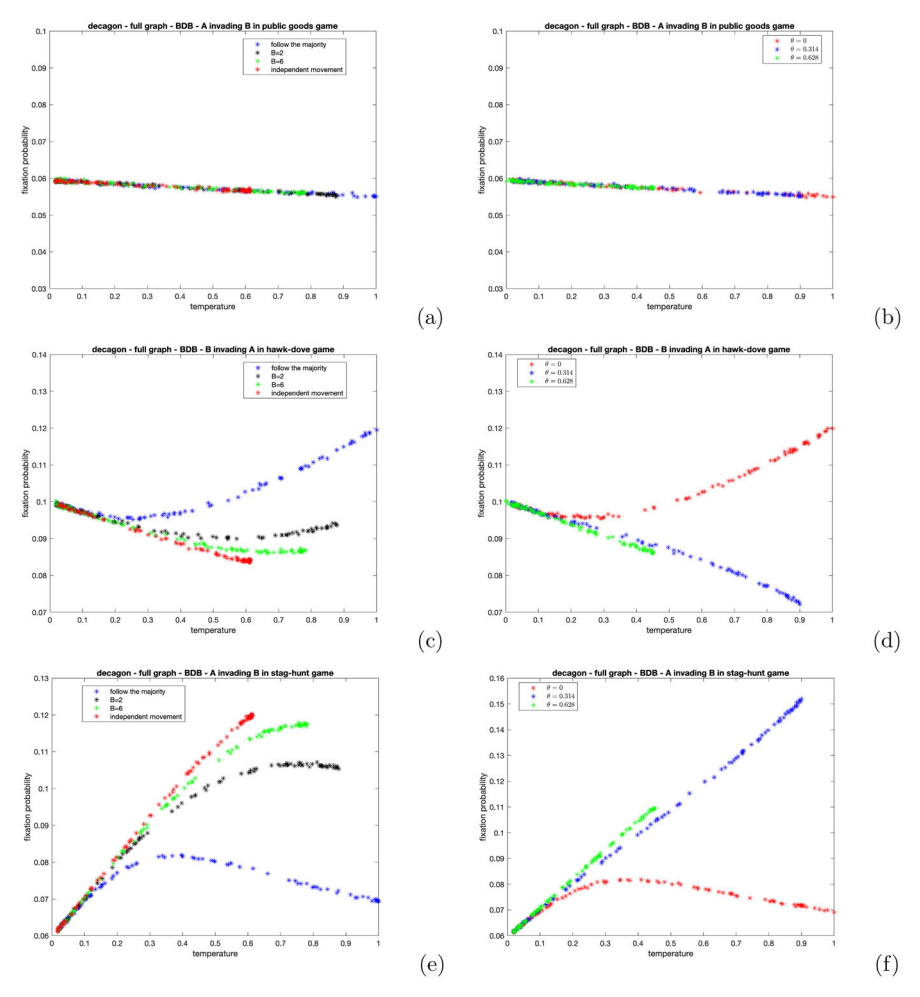


Fig. 6 The fixation probability plotted against the temperature for a well-mixed population in the Public Goods, Hawk-Dove and Stag-Hunt games on the complete decagon graph. As we vary h, we plot the corresponding fixation probability and temperature values against each other. Figures (**a**), (**c**) and (**e**) illustrate Polya-urn processes where we set B=0 (follow the majority), B=2, B=6 and B=10,000 (a sufficiently large value of B representing independent movement). (**b**), (**d**) and (**f**) show wheel processes where we set $\theta=0$ (follow the majority), $\theta=\frac{2\pi}{N}$ (represents a near complete dispersal process) and $\theta=\frac{\pi}{N}$

urn increases. The trends in Fig. 4b for the wheel process are largely similar to the Polya-urn, except when the angle between the spikes is approximately $\frac{2\pi}{N}$ and h=1. At this point, all individuals within the population are nearly always alone. Given the significant effects of the movement processes on the mean group size, we considered the impact of mean group size on the fixation probability of cooperative strategies, as shown in Fig. 5.

Figure 5 illustrates the fixation probabilities of cooperative strategies plotted against the mean group size under the Polya-urn and wheel processes on the complete decagon. Figure 5a and b show the fixation probability of a mutant cooperator in the public goods game. As the mean group size increases, the cooperator's fixation probability decreases for all movement processes. This result is expected, as larger group sizes lead to interactions between coop-



erators and defectors, allowing defectors to gain rewards and thereby reducing the relative fitness of cooperators. Figure 5c and d depict the fixation probability of a mutant dove. In contrast, as the mean group size increases, the fixation probability also increases. This occurs because hawks are more likely to be grouped together as the group size grows, causing them to endure greater costs, which lowers their relative fitness and, consequently, raises the dove's fixation probability. Figure 5e and represent the cooperator's fixation probability in the staghunt game. Initially, as the mean group size increases, the fixation probability rises until the mean group size reaches the threshold level (set as L=2). This benefits cooperators, as they either find themselves in groups with another cooperator, enabling them to produce and share the reward, or with a defector, in which case the reward cannot be produced. Other values of L would change the mean group size where the maximum fixation probability occurs, constrained by the group formations of the considered movement process. However, as the mean group size continues to increase, the fixation probability declines. This is because larger group sizes do not provide significant additional benefits to cooperators beyond the threshold level and instead allow defectors to join cooperative groups and receive a share of the reward.

Figure 4c and d show the temperature for various Polya-urn (c) and wheel (d) processes for varying values of h on the complete decagon graph. The trends observed here are very similar to those in Figs. 4a and b, as it has been previously demonstrated that temperature increases with mean group size (Broom et al. [15]). This unsurprisingly holds under the considered movement processes. Low values of h correspond to high levels of movement within the population, therefore when h=1, the temperature is at its highest, as individuals are more likely to be replaced by others due to frequent interactions (except for the case where $\theta=\frac{2\pi}{N}$, as individuals are nearly always alone, the temperature is at its lowest). As h increases, individuals are less likely to move and, therefore, less likely to interact with one another, leading to a decrease in temperature across all of the movement processes.

Figure 6 depicts the fixation probabilities of cooperative strategies plotted against the temperature under the Polya-urn and wheel processes on the complete decagon. Figure 6a and b show the fixation probability of a mutant cooperator in the Public Goods game. As the temperature increases, the cooperator's fixation probability decreases for all movement processes. This is because higher temperatures indicate greater levels of mixing between cooperators and defectors, enabling defectors to gain rewards from cooperators. Notably, the different movement processes overlap, indicating that, regardless of the movement mechanism, the temperature consistently predicts the cooperator's fixation probability. In other words, the temperature is the most significant predictor in the Public Goods evolutionary process.

Furthermore, from Fig. 6c and d, we observe that in the Hawk-Dove game, as the temperature increases, the dove's fixation probability increases. High temperature levels correspond to low values of h and, therefore, high levels of interaction between doves and hawks. As hawks interact with one another, they incur greater costs, which reduces their relative fitness and, consequently, increases the dove's fixation probability. Additionally, the relationship between temperature and the dove's fixation probability is linear for small temperature values but breaks down as temperature increases, particularly for the follow the majority process. Low temperatures, correspond to high values of h, meaning many individuals are not partaking in the movement process and are either alone or in small pairwise groups. As temperature increases, more individuals become mobile, leading to the formation of groups of various sizes, particularly for the follow the majority process, which significantly disadvantages hawks and causes the linearity breakdown. Thus, in the Hawk-Dove game, at higher temperatures, the governing movement process holds an important role in the evolutionary process.

Furthermore, from Fig. 6e and f, we observe that in the Stag-Hunt game, the cooperator's fixation probability increases as the temperature rises, until it reaches a level where the fixation



probability begins to decrease. Low temperature values indicate limited interaction between individuals. Consequently, the relationship between temperature and fixation probability is linear, similar to that observed in the Hawk-Dove game. As temperature increases, individuals are more likely to move and interact in pairwise groups, when cooperators interact with at least one other cooperator, they can produce the reward, leading to an increase in fixation probability. When B=0 or $\theta=0$, the fixation probability declines rapidly as temperature rises, due to the deterministic nature of the movement process, which causes individuals to herd together. This herding effect is disadvantageous to cooperators, reducing their relative fitness and, consequently, their fixation probability. When $B\neq 0$ or $\theta\neq 0$, the decrease in fixation probability is more gradual, as cooperators move probabilistically and can still engage in beneficial pairwise interactions.

5 Discussion

In this paper, we have extended the modelling framework developed in Broom and Rychtar [14], by utilising the evolutionary model introduced in Haq et al. [31] to not only examine the effects of row-dependent movement (Broom et al. [30]) on predictors of fixation probability, but also to implement the multiplayer Stag-Hunt game within the evolutionary context of the territorial raider model. In previous models, (Broom et al. [15]; Pattni et al. [25]; Schimit et al. [26]) individuals moved independently, meaning that only random movement was considered in the prior analysis of predictors of fixation probability. Also, individuals primarily interacted via the Public Goods, Hawk-Dove or Fixed Fitness Games. We have considered a different social dilemma in the form of the multiplayer Stag-Hunt game, where selection can favour the evolution of cooperation depending on the movement mechanism governing the process (unlike in the Public Goods game, where cooperation cannot evolve in well-mixed populations).

We first demonstrated in Sect. 4.1 how previously defined measures of aggregation from Broom et al. [30], specifically T (15) relate to the mean group size and showed how T, mean group size and temperature can be calculated. Previous work by Broom et al. [15] and Schimit et al. [26] explained the importance of these predictors, and our aim was to demonstrate that these measures not only hold theoretical significance, but can also be practically calculated for various movement processes. In Sect. 4.2, we examined the Stag-Hunt game and showed that herding can be significantly detrimental to the evolution of cooperation, to the extent that selection opposes its evolution. However, other movement processes raise the cooperator's fixation probability above that of the defector and above the neutral benchmark, thereby supporting the evolution of cooperation. A significant example of this was shown in the wheel process. In the Stag-Hunt game, row-dependent movement plays a more influential role than in the Public Goods game considered by Haq et al. [31]. Dispersal can also be detrimental to cooperators as it ensures cooperators partaking in the movement process, do not interact with each other, reducing their chances of being in a group that meets the threshold.

We also considered the effects of various movement processes on the mean group size and temperature and, in turn, their influence on fixation probability and have observed patterns in our model that have not been previously observed in evolutionary graph theory (Pattni et al. [39] and Traulsen et al. [40]). In the Public Goods game, we demonstrated that temperature is a stronger predictor of fixation than mean group size across all levels of h, regardless of the movement process. Our findings indicated that temperature maintains a linear relationship



with fixation probability for all movement processes, signifying its importance as the most crucial parameter in the evolutionary process. This was first identified by Broom et al. [15] but only for high levels of home fidelity and independent movement. Our analysis extends this work by incorporating more complex movement mechanisms, demonstrating that temperature's predictive property remains robust even when individuals move in a coordinated manner. In the Hawk-Dove game, we showed that temperature continues to be a stronger predictor of fixation. However, due to the greater complexity of the game compared to the public goods game, the linear relationship between temperature and fixation breaks down as the temperature rises, with a similar pattern observed in the Stag-Hunt game. We provided an analytical analysis of this relationship, highlighting that while temperature is generally a reliable predictor, the nature of the game and the governing movement process play significant roles in determining the relationship between temperature and fixation.

There are several directions for future work. Previous research by Schimit et al. [26] investigated predictors of fixation probability in the context of complex graph structures, where individuals did not reside within well-mixed populations. Since our aim was to extend the analysis carried out by Haq et al. [31], which focused exclusively on complete networks and row-dependent movement mechanisms, the analysis in this paper is also limited to complete graphs. We intend to address this limitation by exploring non-complete graph structures to examine not only the effects of coordinated movement on fixation, but also the influence of the key predictors discussed in this paper. Another potential direction could involve investigating the effects of row-dependent movement within the context of the generalised territorial raider model developed by Pattni et al. [25], which accommodates more complex evolutionary models, where individuals reside within subpopulations. Alternatively, new movement mechanisms could be explored where individuals move to places containing the largest number of cooperators. However, similar movement distributions are already characterised in other versions of the territorial raider model that consider history-dependent movement (Pattni et al. [28]; Erovenko et al. [29]; Pires et al. [41]; Erovenko et al. [33]), where individuals prefer to remain within groups that enhance their fitness. A more complex avenue would involve the simultaneous consideration of row-dependent and history-dependent movement.

Appendix

Mean group size calculation

When we calculated the mean group size under independent movement, we considered a process where L individuals partake in the movement process. These individuals can either move to an empty place or to a place already containing an individual that did not move. The mean group size under independent movement is given by

$$|G| = \sum_{L=0}^{N} \left(\frac{L}{N} \sum_{j=0}^{L} \left(\frac{1}{N}\right)^{j} \left(\frac{N-1}{N}\right)^{L-j} {L \choose j} (j)^{2} + \left(1 - \frac{L}{N}\right) \sum_{j=0}^{L} \left(\frac{1}{N}\right)^{j} \left(\frac{N-1}{N}\right)^{L-j} {L \choose j} (j+1)^{2} (\lambda)^{L} (1-\lambda)^{N-L} {N \choose L}.$$

By expanding the summations and simplifying, we have

$$|G| = 1 + \lambda \left(2 - \frac{1}{N}(2 + \lambda N - \lambda)\right). \tag{31}$$

Therefore, by using (19), T, under independent movement is given by

$$T = \frac{1}{N-1}\lambda \left(2 - \frac{1}{N}(2 + \lambda N - \lambda)\right). \tag{32}$$

For the wheel process, we first calculated T (15) and then used (19) to then determine the mean group size. In an N-sized, well-mixed population, there are the various ways I_i and I_j can be together. For instance, I_i and I_j may both partake in the movement process and move to the same place. Alternatively, I_i may partake in the movement process and move to I_j 's home vertex, while I_j does not partake in the movement process and remains on their home vertex, or vice versa.

$$\begin{split} P(I_i \text{ and } I_j \text{ are together}) &= \sum_{L=2}^{N-1} \sum_{j=1}^{j_m} (L-j) (1 - \frac{\theta j N}{2\pi}) (\lambda)^L (1-\lambda)^{N-L} \binom{N-2}{L-2} \\ &+ \sum_{L=1}^{N} (2) (\lambda)^L (1-\lambda)^{N-L} \binom{N-2}{L-1} (\frac{1}{N}). \end{split}$$

The first summation represents the probability of individuals I_i and I_j of distance j spikes, being together at the same place and $j_m = \min(\lfloor \frac{2\pi}{N\theta} \rfloor, r)$ represents the cut-off point where this no longer holds. By expanding the summations and simplifying, T is given by

$$T = \frac{1}{N(N-1)} \left(\left(\sum_{\frac{2\pi}{N\theta}}^{N} ((\frac{2\pi}{N\theta})^2 + \frac{1}{2} ((\frac{2\pi}{N\theta})^2 + \frac{2\pi}{N\theta}) \left(\frac{N\theta}{2\pi} (1 - \frac{2\pi}{N\theta}) - 1 \right) + \sum_{L=2}^{\frac{2\pi}{N\theta}-1} \left(L^2 + \frac{L^2 + L}{2} (\frac{N\theta}{6\pi} (1 - L) - 1) \right) \right) (\lambda)^L (1 - \lambda)^{N-L} \binom{N-2}{L-2} + \frac{2(\lambda - \lambda^2)}{N} \right).$$
(33)

Therefore, by using (19), the mean group size is

$$|G| = 1 + \frac{1}{N} \left(\left(\sum_{\lfloor \frac{2\pi}{N\theta} \rfloor}^{N} \left(\left(\lfloor \frac{2\pi}{N\theta} \rfloor \right)^{2} + \frac{1}{2} \left(\left(\lfloor \frac{2\pi}{N\theta} \rfloor \right)^{2} + \lfloor \frac{2\pi}{N\theta} \rfloor \right) \left(\frac{N\theta}{2\pi} (1 - \lfloor \frac{2\pi}{N\theta} \rfloor) - 1 \right) \right.$$

$$\left. + \sum_{L=2}^{\lfloor \frac{2\pi}{N\theta} \rfloor - 1} \left(L^{2} + \frac{L^{2} + L}{2} \left(\frac{N\theta}{6\pi} (1 - L) - 1 \right) \right) (\lambda)^{L} (1 - \lambda)^{N-L} \binom{N-2}{L-2} + \frac{2(\lambda - \lambda^{2})}{N} \right).$$

$$(34)$$

Temperature calculations

When calculating the temperature of an individual under independent movement, it was simpler to consider the probability of an individual being alone, as the temperature is also equal to 1-P(alone). In an N-sized, well-mixed population, there are various ways I_i can be alone. For instance, I_i may not partake in the movement process, remain on their home vertex and have no one else move to the same place. Alternatively, I_i may partake in the movement process, move to their home vertex, and find themselves alone, with no other individuals moving to the same vertex. Another possibility is that I_i and I_j both partake in the movement process, I_i moves to I_j 's home vertex, and is alone, provided no other individuals move to the same place.



$$P(I_i \text{ is alone}) = \sum_{L=0}^{N-1} (\lambda)^L (1-\lambda)^{N-L} \binom{N-1}{L} \left(1 - \frac{1}{N}\right)^L + \sum_{L=2}^{N} (\lambda)^L (1-\lambda)^{N-L} \binom{N-2}{L-2} \left(\frac{N-1}{N}\right) \left(1 - \frac{1}{N}\right)^{L-1} + \sum_{L=1}^{N} (\lambda)^L (1-\lambda)^{N-L} \binom{N-1}{L-1} \left(\frac{1}{N}\right) \left(1 - \frac{1}{N}\right)^{L-1}.$$

Expanding the summations and simplifying,

$$P(I_i \text{ is alone}) = \frac{N(N + N\lambda(\lambda - 1) - \lambda^2)(N - \lambda)^{N-2}(1 - \lambda)^N}{(N - N\lambda)^N}.$$

Therefore, the temperature under independent movement is given by

$$\tau_N = 1 - \frac{(N + N\lambda(\lambda - 1) - \lambda^2)(N - \lambda)^{N - 2}}{N^{N - 1}}.$$
 (35)

Using a similar approach to calculate the temperature for the wheel, we considered θ in two possible ranges $0 \le \theta \le \frac{\pi}{N}$ and $\frac{\pi}{N} \le \theta \le \frac{2\pi}{N}$ as this includes the cases where all spikes can aggregate, to complete separation. Consider individual I_i where $0 \le \theta \le \frac{\pi}{N}$:

- I_i partakes in the wheel process and moves to their home vertex and no one else joins
- I_i partakes in the wheel process and moves to someone else's vertex, alone.
- I_i does not partake in the wheel process and stays on their home vertex, alone.
- No one in the population partakes in the movement process, therefore I_i remains alone.

$$P(I_i \text{ is alone}) = \frac{1}{N}(N-1)(1-\lambda)((1-\lambda)^{N-1}-1) + (1-\lambda)^N + \frac{\theta}{\pi} \left(\lambda + \frac{1}{2}((1-\lambda)(1-(1-\lambda)^{N-1}) + (N-1)(\lambda-1)(\lambda))\right).$$

By expanding the summations and simplifying, the probability of being alone is

$$T_N = 1 - \left(\frac{1}{N}(N-1)(1-\lambda)(1-(1-\lambda)^{N-1}) + (1-\lambda)^N + \frac{\theta}{\pi}\left(\lambda + \frac{1}{2}((1-\lambda)(1-(1-\lambda)^{N-1}) + (N-1)(\lambda-1)(\lambda))\right)\right)$$

and, therefore, the temperature for $0 \le \theta \le \frac{\pi}{N}$ is given by

$$T_{N} = 1 - \left(\frac{1}{N}(N-1)(1-\lambda)(1-(1-\lambda)^{N-1}) + (1-\lambda)^{N} + \frac{\theta}{\pi}\left(\lambda + \frac{1}{2}((1-\lambda)(1-(1-\lambda)^{N-1}) + (N-1)(\lambda-1)(\lambda))\right)\right).$$
(36)

By using very similar methods, the temperature for $\frac{\pi}{N} \le \theta \le \frac{2\pi}{N}$ is given by

$$\tau_{N} = 1 - \left(\frac{1}{N} \left(-1 + (1 - \lambda)^{N} + \lambda(\lambda + 2) - N(\lambda^{2} + \lambda - 1) \right) - \frac{\theta}{2\pi} \left(-1 + (1 - \lambda)^{N} + \lambda(N + 3\lambda - 3N\lambda) \right) \right).$$
(37)



Acknowledgements This work would not have been possible without the funding provided by the studentship awarded to Hasan Haq by City St George's, University of London and PHTS acknowledges the support of the National Council for Scientific and Technological Development (CNPq), grant #421779/2022-5, and the São Paulo Research Foundation (FAPESP), grant #2022/16196-0. This project has received funding from the European Union's Horizon 2020 research and innovation programme under the Marie Sklodowska-Curie grant agreement No 955708. We also acknowledge the use of the high-performance computing system (Hyperion) at City St George's, University of London, which was instrumental in carrying out the simulations presented in this paper.

Author Contributions H.H. and M.B. contributed to the analytical and numerical analysis. Computational development was carried out by P.S. The original draft was prepared by H.H., with editing contributions from H.H. and M.B. The review process involved H.H., M.B., and P.S. Funding was secured by H.H., M.B., and P.S.

Data Availability No datasets were generated or analysed during the current study.

Declarations

Conflict of interest The authors declare that they have no Conflict of interest.

Open Access This article is licensed under a Creative Commons Attribution 4.0 International License, which permits use, sharing, adaptation, distribution and reproduction in any medium or format, as long as you give appropriate credit to the original author(s) and the source, provide a link to the Creative Commons licence, and indicate if changes were made. The images or other third party material in this article are included in the article's Creative Commons licence, unless indicated otherwise in a credit line to the material. If material is not included in the article's Creative Commons licence and your intended use is not permitted by statutory regulation or exceeds the permitted use, you will need to obtain permission directly from the copyright holder. To view a copy of this licence, visit http://creativecommons.org/licenses/by/4.0/.

References

- 1. Lieberman E, Hauert C, Nowak M (2005) Evolutionary dynamics on graphs. Nature 433(7023):312–316
- 2. Maynard Smith J (1982) Evolution and the theory of games. Cambridge University Press, Cambridge
- 3. Antal T, Scheuring I (2006) Fixation of strategies for an evolutionary game in finite populations. Bull Math Biol 68(8):1923–1944
- Broom M, Rychtar J (2008) An analysis of the fixation probability of a mutant on special classes of non-directed graphs. Proc Roy Soc London A 464:2609–2627
- 5. Maciejewski W (2014) Reproductive value in graph-structured populations. J Theor Biol 340:285–293
- Hindersin L, Traulsen A (2014) Counterintuitive properties of the fixation time in network-structured populations. J Royal Soc Interface 11(99):20140606
- 7. Cuesta FA, Sequeiros PG, Rojo AL (2017) Suppressors of selection. PLOS One 12(7):e0180549
- Santos FC, Pacheco JM (2006) A new route to the evolution of cooperation. J Evol Biol 19(3):726–33. https://doi.org/10.1111/j.1420-9101.2005.01063.x
- Broom M, Hadjichrysanthou C, Rychtar J (2010) Evolutionary games on graphs and the speed of the evolutionary process. Proc Royal Soc A 466:1327–1346
- Li C, Zhang B, Cressman R, Tao Y (2013) Evolution of cooperation in a heterogeneous graph: fixation probabilities under weak selection. PloS one 8(6):e66560
- Voorhees B (2013) Birth-death fixation probabilities for structured populations. Proc R Soc A Math Phys Eng Sci 469(2153):20120248
- Tkadlec J, Pavlogiannis A, Chaterjee K, Nowak MA (2020) Limits on amplifiers of natural selection under death-birth updating. PLOS Computat Biol 16(1):e1007494
- Fic M, Gokhale CS (2024) Catalysing cooperation: the power of collective beliefs in structured populations. npj Complex. https://doi.org/10.1038/s44260-024-00005-z
- Broom M, Rychtar J (2012) A general framework for analysing multiplayer games in networks using territorial interactions as a case study. J Theor Biol 302:70–80
- Broom M, Lafaye C, Pattni K, Rychtar J (2015) A study of the dynamics of multi-player games on small networks using territorial interactions. J Math Biol 71:1551–1574



- Broom M, Pattni K, Rychtar J (2018) Generalized social Dilemmas: the evolution of cooperation in populations with variable group size. Bullet Math Biol. https://doi.org/10.1007/s11538-018-00545-1
- 17. Palm G (1984) Evolutionary stable strategies and game dynamics for n-person games. J Math Biol 19(3):329–334
- 18. Broom M, Cannings C, Vickers GT (1997) Multi-player matrix games. Bullet Math Biol 59:931–952
- Bukowski M, Miekisz J (2004) Evolutionary and asymptotic stability in symmetric multi-player games. Int J Game Theory 33(1):41–54
- Ohtsuki H, Hauert C, Lieberman E, Nowak M (2006) A simple rule for the evolution of cooperation on graphs and social networks. Nature 441(7092):502–505
- Santos F, Santos M, Pacheco J (2008) Social diversity promotes the emergence of cooperation in public goods games. Nature 454(7201):213–216
- 22. van Veelen M, Nowak M [2012] Multi-player games on the cycle. J Theor Biol 292:116-128
- Hadjichrysanthou C, Broom M, Rychtář J (2011) Evolutionary games on star graphs under various updating rules. Dyn Games Appl 1(3):386–407
- 24. Broom M, Rychtar J (2013) Game-Theor Models Biol. CRC Press, Boca Raton
- Pattni K, Broom M, Rychtar J (2017) Evolutionary dynamics and the evolution of multiplayer cooperation in a subdivided population. J Theor Biol 429:105–115
- Schimit PHT, Pattni K, Broom M (2019) Dynamics of multiplayer games on complex networks using territorial interactions. Phys Rev E. https://doi.org/10.1103/physreve.99.032306
- Schimit PHT, Pereira FH, Broom M (2022) Good predictors for the fixation probability on complex networks of multi-player games using territorial interactions. Ecol Complex 51:101017–101017. https:// doi.org/10.1016/j.ecocom.2022.101017
- Pattni K, Rychtar Broom MJ (2018) Evolving multiplayer networks: modelling the evolution of cooperation in a mobile population. Discrete Contin Dyn Syst B 23:1975–2004
- Erovenko IE, Bauer J, Broom M Pattni K Rychtar J (2019) The effect of network topology on optimal exploration strategies and the evolution of cooperation in a mobile population. In: Proceedings of the royal society of London A 47520190399
- Broom M, Erovenko IV, Rowell JT, Rychtar J (2020) Models and measures of animal aggregation and dispersal. J Theor Biol 494:110002
- 31. Haq H, Schimit PHT, Broom M (2024) The effects of herding and dispersal behaviour on the evolution of cooperation on complete networks. J Math Biol 89:49. https://doi.org/10.1007/s00285-024-02148-y
- Broom M, Erovenko I, Rychtar J (2021) Modelling evolution in structured populations involving multiplayer interactions. Dyn Games Appl 11:270–293
- Erovenko IV, Broom M (2024) The evolution of cooperation in a mobile population on random networks: network topology matters only for low-degree networks. Dyn Games Appl. https://doi.org/10. 1007/s13235-024-00572-9
- Nowak M (2006) Evolutionary dynamics, exploring the equations of life. Harward University Press, Cambridge
- 35. Taylor C, Fudenberg D, Sasaki A, Nowak M (2004) Evolutionary game dynamics in finite populations. Bullet Math Biol 66(6):1621–1644
- 36. Karlin S, Taylor H (1975) A first course in stochastic processes. Academic Press, London
- Johnson NL, Kotz S (1977) Urn models and their application; an approach to modern discrete probability theory. Wiley, New York
- Gabor Csardi, Tamas Nepusz (2006) The igraph software package for complex network research. InterJ Complex Syst 1695:1–9
- Pattni K, Broom M, Rychtar J, Silvers AJ (2015) Evolutionary graph theory revisited: when is an evolutionary process equivalent to the Moran process? Proc Royal Soc A 471(2015):0334
- Traulsen A, Nowak MA, Pacheco JM (2007) Stochastic payoff evaluation increases the temperature of selection. J Theor Biol 244(2):349–56. https://doi.org/10.1016/j.jtbi.2006.08.008
- Pires DL, Erovenko IV, Broom M (2023) Network topology and movement cost, not updating mechanism, determine the evolution of cooperation in mobile structured populations. PLoS One 18(8):0289366

Publisher's Note Springer Nature remains neutral with regard to jurisdictional claims in published maps and institutional affiliations.

